Response of a Pool-type LMR to Seismic Loads*

C. Y. Wang and J. Gvildys
Reactor Analysis and Safety Division, Argonne National Laboratory,
Argonne, Illinois 60439 USA

CONF-890855--53

DE89 017699

*Work supported by the U.S. Department of Energy, Office of Technology Support Program, under Contract W-31-109-Eng-38.

INTRODUCTION

This paper describes the seismic analysis of a 450-MWe pool-type liquid metal reactor (LMR) under 0.3 g SSE ground excitations. It also assess the ultimate inelastic structural capabilities for other beyond-design-basis seismic events. Calculation is focused on a new design configuration where the vessel thickness is reduced considerably compared to the previous design (Ma and Gvildys, 1987). In the analysis, the stress and displacement fields at important locations of the reactor vessel, guard vessel, and support skirt are investigated. Emphasis is placed on the horizontal excitation in which large stress is generated. The possibility of impact between the reactor and guard vessels is examined. In the reactor vessel analysis, the effect of fluid-structure interaction is included. Attention is further given to the maximum horizontal acceleration of the reactor core as well as the relative displacement between the reactor core and the upper internal structure.

The Argonne National Laboratory augmented three-dimensional Fluid-Structure Interaction program, FLUSTR-ANL (Chang et al, 1988) is utilized for performing the base calculation where ground excitation is assumed to be 0.3 g SSE. The Newmark-Hall Ductility modification method was used for the beyond-design-basis seismic events. In both calculations, stress fields generated from the horizontal and vertical excitations are evaluated separately. The resultant stresses due to combined actions of these events are computed by the SRSS method.

THE MATHEMATICAL MODEL

To conserve the computer core storage and to save the computational cost separate calculations are performed for the reactor vessel, the guard vessel and support skirt. Also, different models are used depending on the directions of the seismic excitation. A 3-D model is chosen for the horizontal excitation analysis, whereas a simplified axisymmetric model is developed for the vertical excitation calcu 'ion. Moreover, in the analysis of the guard vessel and support skirt, the reactor vessel and its internals are simulated by beam elements in which coolant and component masses are appropriately lumped at element ' 'al points.

To facilitate the numerical calculation, a 180° sector of the finite element Model is developed for the horizontal excitation analysis. Figures 1 and 2

---

*Work performed under the auspices of the U.S. Department of Energy, Office of Technology Support Program, under Contract W-31-109-ENG-38.

provide the computer-generated plots describing the isoparametric and elevation views of the LMR. In the analysis, the fluid is simulated by the eight nodes fluid element. The RV and redan are represented by the resultant stress Degenerated Shell (RSDS) elements. Major in-tank components, thermal liner, skirt extension of the shield barrel, and the core-support structure (including the shield barrel and core-support cylinders) are approximated by beam elements.

Since in this detailed 3-D analysis the response of the RV and major components are calculated simultaneously by solving the fluid and structural governing equations, the effect of fluid-structure interaction is appropriately considered. This is quite different from the conventional lump-mass technique, where the reactor vessel is represented by a stick or a shell, and no fluid-structure coupling calculation is considered.

RESULTS

Based on the computed stress components, the equivalent stress of each shell element is obtained. This stress represents the magnitude of the stress tensor at a given location. It represents the local stress level and has the form (Mendelson, 1968)

$$\sigma_e = \frac{1}{\sqrt{2}} [(\sigma_x - \sigma_y)^2 + (\sigma_y - \sigma_z)^2 + (\sigma_z - \sigma_x)^2 + 6 (\sigma_{xy}^2 + \sigma_{yz}^2 + \sigma_{zx}^2)]^{1/2} \quad , \tag{1}$$

in which σ_x, σ_y, and σ_z are normal stresses with respect to three orthogonal axes; σ_{xy}, σ_{yz}, and σ_{zx} are the shearing stresses. Once the equivalent stress is calculated, it can be used to compare with the material yield and/or ultimate stresses to determine the characteristic of the subsequent structural response.

Elastic structural capability is of importance since within this limit no permanent deformation and structural damage will occur. To determine the maximum ZPA of ground excitation corresponding to the material yield strength, stress fields at several critical locations are presented here. The maximum equivalent stresses due to both horizontal and vertical seismic events are calculated by the SRSS method.

Table 1 gives the maximum equivalent stresses at important locations along the reactor vessel (see Fig. 1), i.e., at elements 1 (first row, 0° location), 9 (first row, 90° location), 17 (first row, 170° location), 27 (second row, 90° location), 156 (near junction of RV and baffle plate), 217 (vessel-lower head junction), and 378 (RV-CSS junction, 90° location). It can be seen that the equivalent stress generated from the combined action of the three stress components is about 8700 psi. This value is considerably smaller than the material yield stress of 17,000 psi (SS 316 annealed). The ratio of the maximum equivalent stress to the material yield stress is about 1.0 to 1.95. This implies that for the new reactor design, the response of the reactor vessel will remain in the elastic regime if the ground excitation has a ZPA of 0.586 g. For illustration of the horizontal-excitation analysis, the hoop stress near vessel-lower head junction and axial stress near the upper vessel as well as their FFT are presented in Fig. 3 and 4, respectively.

Similarly, equivalent stresses at several locations of the support skirt and guard vessel are presented in Table 2. These include locations of 3-D model corresponding to elements 127 and 132 (90° location) of the upper skirt, 115 and 120 of the lower skirt, as well as element 109 (90° location) of the upper guard vessel. Figure 5 shows the axial stress and its FFT at lower skirt under vertical excitation.

It is found that the maximum equivalent stress is abut 2,030 psi, which occurs at the upper support skirt and is far below the material yield stress of 26,000 psi (316 SS annealed at 260°F). The ratio of the maximum equivalent stress to the material yield stress is about 1.0 to 12.80. This means that without the presence of sodium in the annular region between the reactor and guard vessels, the response of the guard vessel and support skirt will remain in the elastic regime even if the ground excitation has a ZPA of 3.84 g. Thus, we believe that considerable design conservatism has been provided for the new reactor design.

INELASTIC STRUCTURAL CAPABILITIES

Because of the material nonlinearity and its energy-absorption capability the reactor components generally can withstand more severe seismic events than those mentioned in the previous section. The energy absorption in the inelastic range is handled by the so called "ductility ratio" (Newmark and Hall, 1978). It is defined by

$$\mu = \frac{u_m}{u_y} , \quad (2)$$

where u_m and u_y are the ultimate and effective elastic displacements, respectively.

In general, for small displacements into the inelastic range when the latter is approximated by an elasto-plastic resistance curve, the response spectrum is decreased by a factor which is one over the ductility ratio for the frequency less than 2.0 Hz and a factor of $1/\sqrt{2\mu-1}$ for frequency between 2.0 and 8.0 Hz. There is no reduction for frequency beyond 33.0 Hz.

Here, we assume that such a scheme is also applicable to the time-history method. Furthermore, we assume that both the reactor and component belong to the class-II structures (Newmark and Hall, 1978) which have a ductility ratio of 2.0 - 3.0. Thus, one can shown that the factor of acceleration reduction is about 1.732 to 2.236 based on μ=2.0-3.0. Modifying this factor to the beyond-design-basis seismic events of the reactor and guard vessels (0.59 g and 3.84 g respectively) it is seen that the RV and guard vessel can withstand beyond-design-basis seismics with peak accelerations ranging from 1.01-1.31 g and 6.65-8.59 g, respectively. These correspond to 3.37-4.37 times the 0.3 g SSE for the reactor vessel, and 22.17-28.63 times the basic 0.3 g SSE for the guard vessel (no sodium) and support skirt.

CONCLUSIONS

Seismic analysis has been performed for the new design of the 450-MWe pool-type LMR subjected to both horizontal and vertical excitations. Several remarks can be drawn from this study:

1. The dominant frequency of the reactor vessel subjected to 0.3-g horizontal SSE is about 7.05 Hz. The maximum stress obtained is 8700 psi, which is still only about half of the material yield stress. The shear effect resulting from the horizontal excitation is the major cause of this stress and accounts for 90% of the total stress. For the guard vessel and support skirt, the stress level is very small.

2. The maximum horizontal acceleration of the reactor core is 0.81 g, and the relative horizontal displacement between the UIS and reactor core is only 0.19 in. Both are well below the design specified limits of 3.5 g and 2.2 in.

3. The relative horizontal displacements between the reactor and guard vessels is 0.15 in, which is far smaller than the 6.75-in nominal annular clearance between these two vessels. Thus, vessel impact will not occur during the 0.3-g SSE horizontal excitation.

4. Moments and forces acting on the in-vessel components under horizontal excitation are also increased slightly in the new design. The variations of these values during the design iterations is are about 15%. Stress fields generated by the seismic moments and forces are found to be quite small.

5. Based on the Newmark-Hall ductility method, it is found that the reactor vessel can withstand seismic events with ground ZPAs ranging from 1.01 to 1.31 g, which corresponds to 3.37 to 4.37 times the [illegible] 0.3-g SSE. Thus, we can conclude that the reactor and guard vessels of the pool-type LMR utilized in the new design are strong enough to resist seismic loads.

REFERENCES

Ma, D.C. and Gvildys, J. Seismic Analysis of a Pool-Type Fast Reactors. 9th SMiRT, Vol. E, pp. 493-498.

Chang, Y. W. et al (1988). Seismic Analysis of LMR Reactor Tanks. Nuclear Engineering and Design, Vol. 106, pp. 19-34.

Mendelson, A. (1968). Plasticity: Theory and Application. The MacMillan Company.

Newmark, N. M. and Hall, W. J. (1978). Development of Criteria for Seismic Review of Selected Nuclear Power Plants. NRC NUREG/CR-0098.

Table 1. Maxiumum Stresses at Various Locations of Reactor Vessel Under Combined SSE Horizontal and Vertical Seismic Excitations

Element No.		Maximum Equivalent Stress (psi)		
3-D Model	Location	Horizontal Excitation	Vertical Excitation	Combined Excitations
1	First row, 0°	4875	1740	5176.2
9	First row, 90°	7789	1740	7981.0
17	First row, 170°	5114	1740	4501.9
27	Second row, 90°	7902	3561	8667.3
156	RV-baffle junction	7803	3578	8584.2
217	RV-lower head junction	4871	2938	5688.4
378	RV-CSS junction	2015	4972	5365.0

Table 2. Maxiumum Stresses at Various Locations of Guard Vessel and Support Skirt Under Combined SSE Horizontal and Vertical Seismic Excitations

Element No.		Maximum Equivalent Stress (psi)		
3-D Model	Location	Horizontal Excitation	Vertical Excitation	Combined Excitations
127	Upper skirt, 0°	405	1471	1525.7
132	Upper skirt, 90°	945	1471	1748.4
115	Lower skirt, 0°	406	1842	1887.2
120	Lower skirt, 90°	845	1843	2027.5
109	Upper vessel, 90°	203	195	281.5

Fig. 1 Isoparametric View of the Reactor Vessel Model

Fig. 2 Elevation View of the Reactor Vessel Model

Fig. 3 Hoop Stress and FFT Near Vessel-Lower Head Junction under Horizontal Excitation

Fig. 4 Axial Stress and FFT Near Upper Vessel under Horizontal Excitation

Fig. 5 Axial Stress and FFT at Lower Skirt under Vertical Excitation

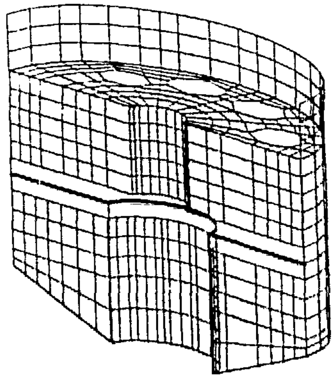

Fig. 1 Isoparametric View of the Reactor Vessel Model

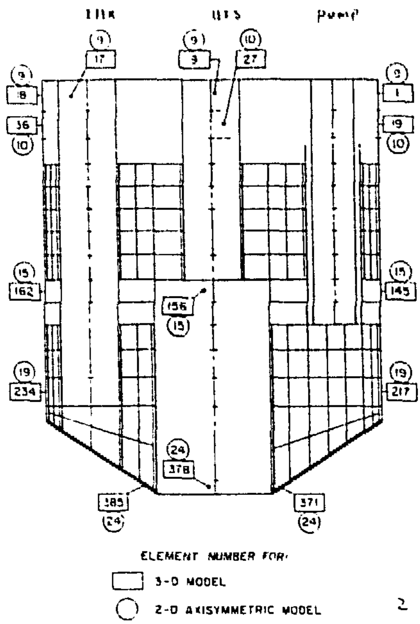

Fig. 2 Elevation View of the Reactor Vessel Model

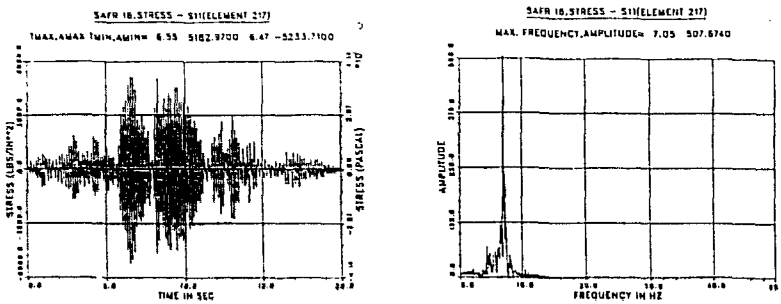

Fig. 3 Hoop Stress and FFT Near Vessel-Lower Head Junction under Horizontal Excitation

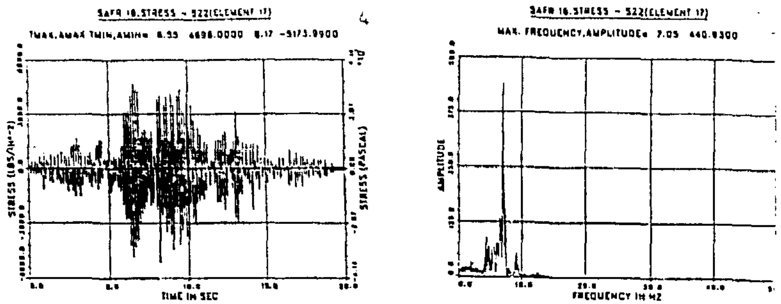

Fig. 4 Axial Stress and FFT Near Upper Vessel Under Horizontal Excitation

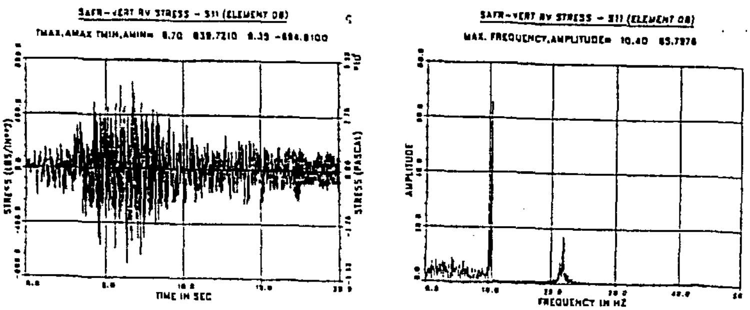

Fig. 5. Axial Stress and FFT at Lower Skirt under Vertical Excitation